

Reversible-growth model: Cluster-cluster aggregation with finite binding energies

Wan Y. Shih, Ilhan A. Aksay, and Ryoichi Kikuchi

Department of Materials Science and Engineering (FB-10), University of Washington, Seattle, Washington 98195

(Received 18 May 1987)

A reversible-growth model is built by modifying the cluster-cluster aggregation model with a finite interparticle attraction energy $-E$. When E is ∞ , the aggregation is described by the ordinary cluster-cluster aggregation model. Within our model, particles as well as clusters are performing Brownian motion according to the rate $1/\tau_D$, and the unbinding takes place according to $(1/\tau_R)e^{-\Delta E/T}$, where ΔE is the energy change due to the unbinding, T is the room temperature, and τ_R is the time constant associated with the unbinding. The Boltzmann constant is taken to be unity. By changing E and τ_R/τ_D , we are able to change the aggregation behavior over a wide range from ramified clusters to compact ones. Moreover, due to a finite E , ramified aggregates may become compact at a later time. We show that the initially fractal aggregates can remain fractal objects during restructuring while the fractal dimension D increases with time. At large E , D can stay at some value that is larger than the value of the cluster-cluster aggregation model and can remain unchanged for a long time. At a given time, D increases drastically with decreasing E from the value of the cluster-cluster aggregation model when $E \leq 3T$. The curve of the estimated sedimentation density versus E resembles that of D versus E and agrees with the experiments.

I. INTRODUCTION

Under suitable conditions, fine colloidal particles ($\sim 50 \text{ \AA} - \sim 1 \text{ \mu m}$ in diameter) can form aggregates of a fairly large size (up to several thousand particles). Extensive light-, x-ray-, and neutron-scattering experiments¹⁻⁶ showed that these aggregates are fractal objects and that the fractal dimension D varies with the experimental condition, $D=1.75$ (Refs. 2, 4, and 6) when the clusters grow rapidly and $D=2.02-2.12$ (Refs. 1, 3, and 5) when the growth is slow. Furthermore, when light scattering measurements were taken repeatedly in a temporal sequence, it was found that aggregates with an initially lower D (1.75) can restructure to a higher D [2.08-2.1 (Ref. 4), 2.4 (Ref. 6)] at a later time. This signifies that the growth processes involve some reversibility. Some critical questions then arise. How do the structures of these aggregates change with time? Do these aggregates remain fractal objects during restructuring? If so, how does the fractal dimension D change with time?

The cluster-cluster aggregation (CCA) model^{7,8} which yields $D=1.78$ (1.4) for $d=3$ ($d=2$), where d is the Euclidean dimension, seems to agree with the colloidal aggregates of rapid growth. When the CCA model is modified with a sticking probability p and when p is approaching zero,⁹ it produces clusters of $D=2.0$ (1.55) for $d=3$ ($d=2$) and is often compared with the aggregates from slow processes. Although Ref. 9 gives a fractal dimension close to that of the colloidal aggregates by slow growth, it cannot account for the restructuring observed in the experiments because of its irreversible nature. Kolb *et al.*¹⁰ have considered a reversible growth model by modifying the CCA model with random bond breaking which yielded $D=2.03$ (1.57) for $d=3$ ($d=2$) at dynamic equilibrium; however, they did not observe the change of D with time.

The purpose of this study is (1) to construct a more realistic reversible growth model which involves the rearrangement of particles from energetic consideration rather than random bond breaking and (2) to investigate the restructuring of aggregates with computer simulations. The direct observation of the colloidal clustering under an optical microscope¹¹ showed that under weakly attractive conditions, a particle can join and leave a cluster repeatedly and that a particle with fewer bonds is more active than one with more bonds. Furthermore, the compaction of a colloidal sediment can occur upon the decrease of the interparticle attraction.¹² These observations plus other flocculation studies¹³ suggest that the interparticle attractions play an important role in aggregation.

II. MODEL

Since the CCA model seems able to describe the colloidal clusters grown from the rapid processes, we build our model by combining the CCA model with a finite nearest-neighbor attraction energy $-E$. The unbinding process is simulated with the Monte Carlo method. For convenience, the calculations are performed for $d=2$. The procedure is as follows. Initially N' particles are placed randomly in an $M \times M$ square lattice with periodic boundary conditions. The particles and the clusters are performing Brownian motion (random walk). After each time interval τ_D , all particles and clusters move one lattice constant. For simplicity, we assume all clusters to have the same mobility since this does not change the scaling properties.^{7,14} When two clusters collide they stick together, forming a larger cluster and then move on as a whole. Moreover, because of its thermal motion a particle can unbind from its neighbors according to the rate $(1/\tau_R)e^{-\Delta E/T}$, where τ_R is the time constant associ-

ated with the unbinding process, T is the room temperature, and ΔE is the energy change due to the unbinding. The Boltzmann constant is taken to be unity. We assume $\Delta E = nE$ where n is the number of neighbors of that particle, one to three in the case of a square lattice. Particles with four neighbors are not allowed to unbind in this case. In practice, the unbinding transition of every particle is examined after each time interval τ_R with a probability $e^{-nE/T}$. If $e^{-nE/T}$ is larger than a random number, the transition is accepted or otherwise rejected. When the unbinding is accepted, the particle moves one lattice constant in one of the rest of the $4-n$ directions at random and the cluster is divided into segments. The resulting number of segments ranges from two to four depending on the number of neighbors bonded to that particle and on the configuration of the cluster before the breakup. For example, the break off of a double-bonded particle in the neck portion of the cluster can result in as many as three segments, namely, one particle and two other parts. Each segment will then diffuse as an independent cluster and will stick to whatever it collides into later on. In our calculations, we do not allow particles or clusters to rotate. However, we do not expect the rotations to affect the scaling properties.¹⁵

By varying E and τ_R/τ_D , we are able to change the growth behavior over a wide range. The CCA model corresponds to a special case when $E = -\infty$. The parameter τ_R is the inverse of the unbinding attempt frequency while τ_D is related to the diffusivity of the particles in the solution and is used in normalizing the time scale. A large τ_R/τ_D may be interpreted as a higher particle mobility relative to relaxation and is analogous to the quenching rate in the glass transition.

III. RESULTS

We show as examples in Fig. 1 three different aggregation conditions initiated with the same number densities but with different values of E and τ_R/τ_D . Figure 1(a) is the case when $E = 1.5T$ and $\tau_R/\tau_D = 0.2$ in which large aggregates can hardly be formed. Figure 1(b) shows the case when $E = 1.5T$ and $\tau_R/\tau_D = 2$ where aggregates are formed but there are still quite a number of particles left in the fluid phase throughout the simulation. In Fig. 1(c), we show the case when $E = 3.5T$ and $\tau_R/\tau_D = 2$ in which almost no free particles are left in the solution and the cluster looks more ramified. Figures 1(a), 1(b), and 1(c) together show the general trend that cluster size increases with increasing E and τ_R/τ_D .

At a given number density, as E decreases, the cluster size decreases and the fluid phase becomes more favored due to more efficient relaxation. In Fig. 2 we show the saturated cluster size as a function of E for three different cases. The fact that the logarithm of the cluster size is linear with E for all cases indicates that the cluster size decreases exponentially with E . This means that the actual aggregates cannot grow to an infinite size because of the finite-coupling energy. Meanwhile, it is worth noting that the cluster size also increases with increasing τ_R/τ_D or particle concentration, both of which

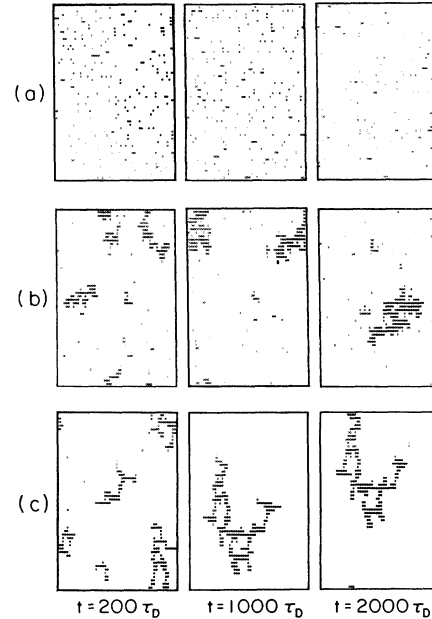


FIG. 1. Temporal evolution of various aggregation conditions with 212 particles in a 50×50 square lattice (a) $E = 1.5T$ and $\tau_R/\tau_D = 0.2$, (b) $E = 1.5T$ and $\tau_R/\tau_D = 2$, and (c) $E = 3.5T$ and $\tau_R/\tau_D = 2$.

are similar to increasing quenching rate. However, we will show later that only E affects the restructuring behavior of clusters with respect to time.

To investigate the effect of restructuring we use two different procedures. (1) We start with clusters of various sizes N grown from the CCA model at the same number density and turn on the relaxation. To show the

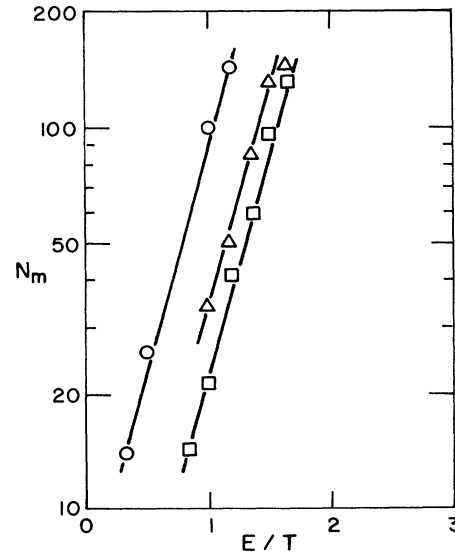


FIG. 2. N_m vs E/T , where N_m denotes the size of the largest cluster, \circ at $\rho = 0.051$, $\tau_R/\tau_D = 5$, Δ at $\rho = 0.125$, $\tau_R/\tau_D = 2$, and \square at $\rho = 0.11$, $\tau_R/\tau_D = 2$ where ρ denotes the number density.

restructuring effect this way is mainly for the ease of comparison, although it may appear unnatural at the first sight (there seems to be a sudden change in E from $-\infty$ to some finite value at $t=0$). What this procedure really represents are the cases where τ_R/τ_D is large enough, i.e., the aggregation is much faster than the relaxation so that initially the aggregates are not very different from those of the CCA model. (2) We have also studied the structural evolution of aggregates during growth. This can be achieved by choosing smaller values of τ_R/τ_D so that sufficient unbinding is taking place along with cluster growth. We will show later that the results of the two procedures are quite similar.

For each set of E and τ_R/τ_D , N is plotted on a log-log scale against R_m in every $100\tau_D$ where R_m is the maximum radius of a cluster and is defined as

$$R_m = \frac{1}{2} \max_{\substack{1 \leq i, j \leq N \\ (i \neq j)}} \{ |r_i - r_j| \} . \quad (1)$$

In each N versus R_m plot, we include 11–14 data points in the range $30 \leq N \leq 200$ –300; each point is the result of averaging over ten samples. It turns out that the curves are linear throughout the simulation and the slope of the lines increases with time. An example done with procedure (1) is given in Fig. 3. Note that for a given N , the corresponding R_m is decreasing with time, indicating that the clusters are getting denser and denser. Note that the $t=500\tau_D$ and the $t=10\,000\tau_D$ plots remain linear while the slope is increasing with time: 1.35 at $t=0$, 1.46 at $t=500\tau_D$, and 1.63 at $t=10\,000\tau_D$. This suggests that the clusters remain fractal during res-

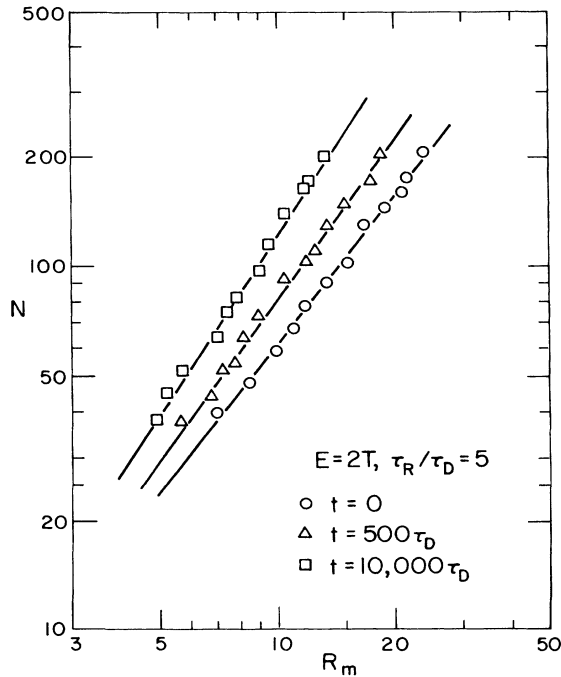


FIG. 3. N vs R_m where N is the cluster size and R_m is the maximum radius in units of the lattice constant as defined in the text.

tructuring but that the fractal dimension is increasing with time.

We then take as the fractal dimension the slope of the $\log N$ versus $\log R_m$ lines by least-square fit. The $t=0$ plot which represents clusters grown from the CCA model thus has a fractal dimension $D=1.35 \pm 0.05$, in agreement with the values obtained in Refs. 7 and 8 within numerical errors. We have also plotted $\log N$ versus $\log R_g$ (not shown) where R_g is the radius of gyration and is defined as

$$R_g = \frac{1}{2N^2} \sum_{\substack{i, j=1 \\ (i \neq j)}}^N |r_i - r_j| . \quad (2)$$

Generally, the fractal dimension D obtained from the $\log N$ versus $\log R_g$ plots are somewhat larger (by about 0.05 on the average) than that of the $\log N$ versus $\log R_m$ plots; however, the difference is comparable with the numerical error bars. The values of D reported in this paper are all based on the N versus R_m plots.

In Fig. 4 we plot D versus t for various values of E and τ_R/τ_D . In Fig. 4(a) we have chosen a small value of

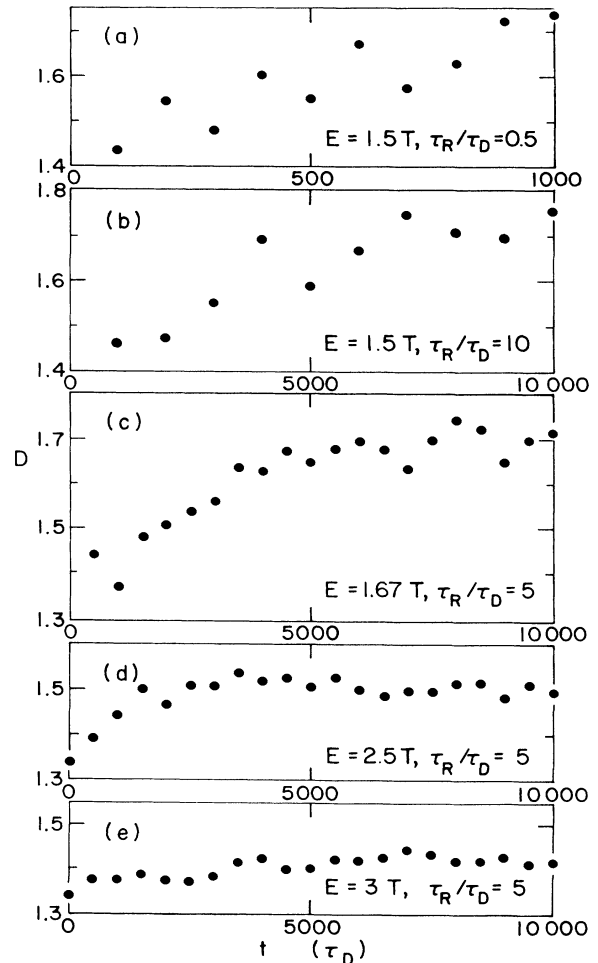


FIG. 4. D vs t for various cases where D is the fractal dimension and t is the time.

$\tau_R/\tau_D=0.5$ and used procedure (2). Because of the small values of τ_R/τ_D and E , the unbinding is taking place sufficiently along with cluster growth. In fact, when we stopped monitoring, i.e., at $t=1000\tau_D$, the clusters were still growing. Thus Fig. 4(a) can be regarded as the structural evolution of aggregates during growth and will be compared with Fig. 4(b) which is obtained by using the same value of E but a different value of τ_R/τ_D and procedure (1). In spite of different procedures used, the two curves look similar and the only difference is in the time units. Thus, varying τ_R/τ_D only changes the time scale but not the behavior of D versus t . When E is increased, the change of D becomes slower, as is shown in Figs. 4(c)–4(e), which are obtained by procedure (1). Note that Figs. 4(d) and 4(e) both have the same value of D which is 1.35 at $t=0$ because we start with the same initial clusters for the purpose of comparison. In Figs. 4(d) and 4(e), D quickly increases from the CCA value and then saturates at some value D' while D' decreases with increasing E : $D'=1.5$ for $E=2.5T$, $D'=1.42$ for $E=3T$. This indicates that under suitable conditions aggregates can have a fractal dimension D that is substantially larger than the CCA value and D remains unchanged over a long period of time, which has been observed experimentally.⁴

We plot in Fig. 5 D versus E for $\tau_R/\tau_D=5$ at $t=5000\tau_D$ and at $t=10000\tau_D$ to show the different restructuring rates at different E . It is clearly shown that the change of D with time is accelerated when E is decreased from $3T$. Also note that for a given t , D remains close to the CCA value at large E but drastically increases from that at around $E \leq 3T$. If we take D as a rough measurement of the densities of the agglomerated solids, we would expect a similarly drastic change in the density when the interaction energy is varied. Indeed, this has been observed in flocculated colloids.¹² We show the relation between the zeta potential of the particles and the sedimentation density in Fig. 6 which is taken from Ref. 12. In a charged colloidal system, the interparticle interaction is the sum of (1) the screened Coulomb repulsion and (2) the van der Waals attraction. The screened Coulomb repulsion can be varied over a

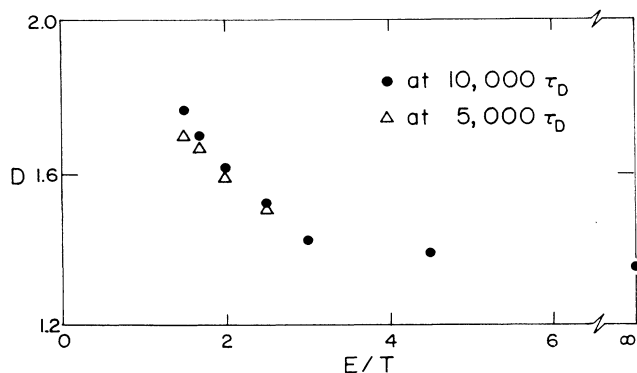


FIG. 5. D vs E for $\tau_R/\tau_D=5$, \circ at $t=10000\tau_D$ and Δ at $t=5000\tau_D$.

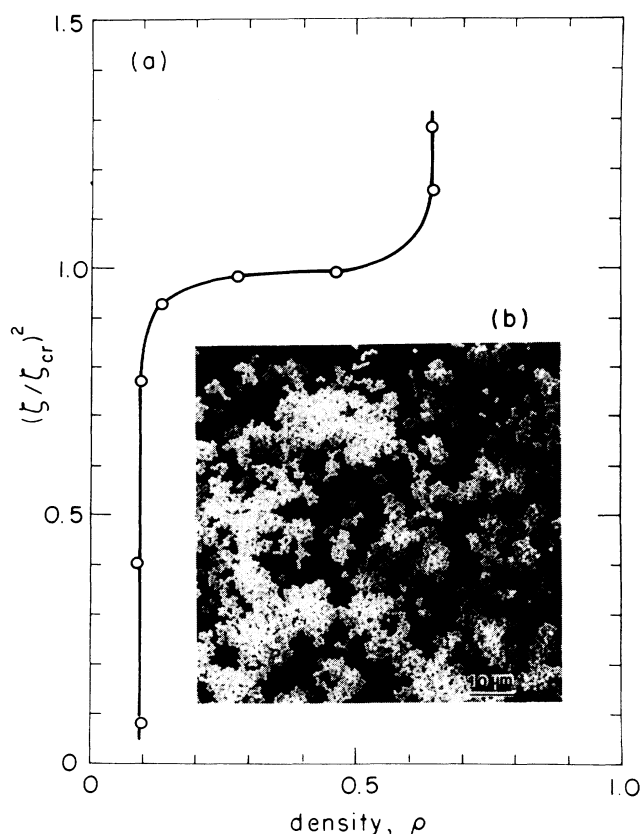


FIG. 6. The variation in the sedimentation density (relative to the total volume) of the colloidal solids as a function of $(\zeta/\zeta_{cr})^2$ where ζ_{cr} is the zeta potential at the critical point.¹² The inset is the scanning electron micrograph of particle clusters formed at low ζ values.

wide range by adjusting the pH, the salt concentration, and so on, while the van der Waals attraction remains more or less unchanged. Thus, under certain pH and salt concentrations, when the screened Coulomb repulsion is sufficiently reduced, a net interparticle attractive potential well can develop. The data points in Fig. 6 were taken under such conditions. The magnitude of the square of the zeta potential ζ^2 can serve as a rough measure of the screen Coulomb repulsion at a fixed salt concentration,¹² the higher the value of ζ^2 , the stronger the Coulomb repulsion. Therefore, in Fig. 6, a smaller value of ζ^2 represents a deeper attraction well. It is shown that at small values of ζ^2 (larger net attractions) the sedimentation density is very low and that the sedimentation density increases at larger values of ζ^2 (smaller net attractions). Note that the sedimentation density does not change much until the zeta potential reaches some critical value ζ_{cr} around which the sedimentation density increases by many folds.

In order to estimate the sedimentation density from our calculations, we assume the sediments to be composed of blobs of some 175 particles and the sedimentation density is approximated to be $175/(\pi R_m^2)$ where R_m is taken from the calculations at $10000\tau_D$. This is not

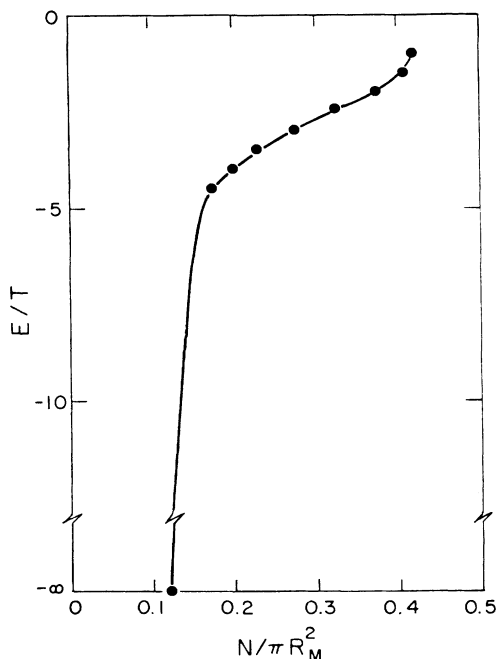


FIG. 7. Estimated sedimentation density vs E . The sediments are assumed to be composed of blobs of some $N=175$ particles and the sedimentation density is approximately to be $N/(\pi R_m^2)$ where R_m is as described in the text.

unreasonable since the aggregates start to settle to the bottom when they reach a certain size. The results are plotted in Fig. 7. One can see that the estimation closely resembles the experimental curve in Fig. 6.

IV. SUMMARY

To summarize, we have built a reversible growth model in which nearest neighbors have a finite attraction energy $-E$ so that the rearrangement of particles is possible. By varying E , τ_R/τ_D , and the particle concentration, we are able to change the aggregation condition

over a wide variety. The restructuring behavior is mainly affected by E . We show that the aggregates can remain fractal during restructuring while the fractal dimension D is increasing with time. When E is large, the change of D becomes so slow that D stays at some intermediate value D' and remains unchanged for a long time while D' decreases with E . In the D versus E plot we show that D increases drastically from the CCA value at around $E \leq 3T$ and is getting closer to d as E is decreased. We have also estimated the sedimentation densities from our calculations. The estimated sedimentation density versus E closely resembles the experimental curve.

In principle, the results we have just shown should readily apply to a variety of systems, since our model is quite general. However, the colloids seem to be ideal to test our results. The reasons are the following. First, the interaction between the colloidal particles can be varied easily over a wide range by changing the particle surface potential (zeta potential), the salt concentration in the solvent, or the extent of steric interaction when they are coated with polymeric units. Second, the size of the colloidal particles can also be varied in a wide range, which is equivalent to changing the particle mobility and is somewhat related to the change of the parameter of τ_R/τ_D in our model.

Note added in proof. J. Liu, M. Sarikaya, W. Y. Shih, and I. A. Aksay¹⁶ have recently been able to grow gold aggregates of various fractal dimensions ranging from 1.75 to ~ 2.7 by coating gold particles with different amounts of surfactants charged with a different sign from that of the gold particles.

ACKNOWLEDGMENTS

The authors would like to thank Wei-Heng Shih for various discussions. This research was supported by the U.S. Air Force Office of Scientific Research (AFOSR) and the Defense Advanced Research Projects Agency (DARPA) of the U.S. Department of Defense and was monitored by the AFOSR under Grant Nos. AFOSR-83-0375 and AFOSR-87-0114.

¹D. A. Weitz, J. S. Huang, M. Y. Lin, and J. Sung, Phys. Rev. Lett. **54**, 1416 (1985).

²D. A. Weitz and M. Olivera, Phys. Rev. Lett. **52**, 1433 (1984).

³D. A. Schaefer, J. E. Martin, P. Wiltzius, and D. S. Cannell, Phys. Rev. Lett. **52**, 2371 (1984).

⁴C. Aubert and D. S. Cannell, Phys. Rev. **56**, 738 (1986).

⁵J. C. Rarity and P. M. Pusey, in *On Growth and Form*, edited by H. E. Stanley and N. Ostrowsky (Nijhoff, Dordrecht, 1986), p. 219.

⁶P. Dimon, S. K. Sinhar, D. A. Weitz, C. R. Safinya, G. Smith, W. A. Varady, and H. M. Lindsay, Phys. Rev. **57**, 595 (1986).

⁷P. Meakin, Phys. Rev. Lett. **51**, 1119 (1983).

⁸M. Kolb, R. Botet, and R. Jullien, Phys. Rev. Lett. **51**, 1123 (1983).

⁹M. Kolb and R. Jullien, J. Phys. (Paris) Lett. **45**, L977 (1984).

¹⁰M. Kolb, R. Botet, R. Jullien and H. J. Herrmann, in *On Growth and Form*, edited by H. E. Stanley and N. Ostrowsky (Nijhoff, Dordrecht, 1986), p. 222.

¹¹G. Y. Onoda, Phys. Rev. Lett. **55**, 226 (1985).

¹²I. A. Aksay and R. Kikuchi, *Science of Ceramic Chemical Processing* (Wiley, New York, 1986), p. 513.

¹³J. A. Long, D. W. J. Osmond, and B. Vincent, J. Colloid Interface Sci. **42**, 545 (1973); C. Cowell and B. Vincent, *ibid.* **518** (1982).

¹⁴P. Meakin, in *On Growth and Form*, edited by H. E. Stanley and N. Ostrowsky (Nijhoff, Dordrecht, 1986), p. 111.

¹⁵P. Meakin, Phys. Rev. A **27**, 604 (1983).

¹⁶J. Liu, M. Sarikaya, W. Y. Shih, and I. A. Aksay (unpublished).

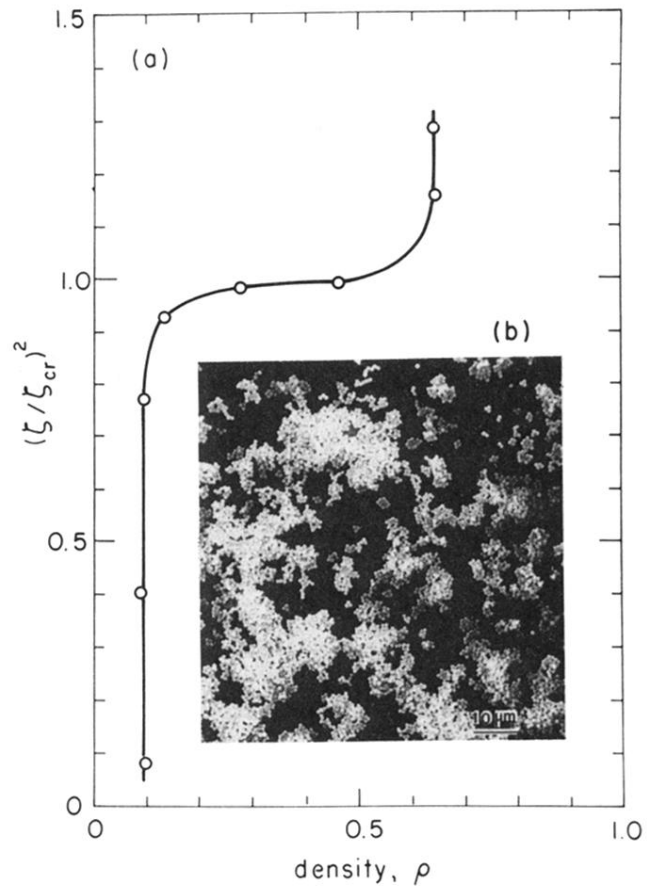


FIG. 6. The variation in the sedimentation density (relative to the total volume) of the colloidal solids as a function of $(\zeta/\zeta_{cr})^2$ where ζ_{cr} is the zeta potential at the critical point.¹² The inset is the scanning electron micrograph of particle clusters formed at low ζ values.